Supporting Information

Hren et al. 10.1073/pnas.1210930110

SI Methods

Age Calibration. Sediments of the Solent Group in the Hampshire Basin, Isle of Wight, United Kingdom were deposited through the Late Eocene to Early Oligocene and span an interval of more than 5 Ma. The timing of deposition of this succession has been well characterized through magnetostratigraphy, sequence stratigraphy, mammalian and charophyte biostratigraphy, and brief calcareous nannoplankton events that allow correlation to the geomagnetic polarity timescale (GPTS) (1–5). Deposition of sediment was relatively rapid (3–10 $cm{\cdot}ky^{-1}$) with the only major hiatus in deposition occurring during the early part of the Oi-1 event in response to major reductions in sea level (1). Such a hiatus is an expected feature of coastal deposits over this interval, although it is shorter than usual in the Hampshire Basin because the high subsidence and sedimentation rate counteracted erosion. Solent Group sediments have been calibrated to the GPTS (1) on the basis of correlation of magnetochrons and sedimentary sequences via marine nannoplankton events and interdigitation of mammal zones with marine zonations elsewhere in Europe according to the timescale of Pälike et al. (6). Calibration to the timescale of data where authors use the Berggren et al. timescale (7) is via tie points, i.e., tops and bases of magnetochrons and the last appearance of the calcareous nannofossil *Discoaster saipanensis*, marking the top of zone NP19–20 [34.43 Ma according to Coxall et al. (8), but 34 Ma according to Pearson et al. (9), using the Berggren et al. (7) timescale]. Intermediate levels are calculated proportionately.

Gastropod Samples. Individual gastropod shells from each interval were analyzed to determine crystal form and the preservation of primary material. Fossil shells from the Eocene to Oligocene Hampshire Basin sections are pristine (Fig. S1), and X-ray diffraction (XRD) analyses of shells from all units are consistent with aragonite. Thin sections of modern *Viviparus* shells show that the shell structure consists of three main layers, the outer prismatic layer, the middle lamellate layer, and the inner nacreous layer (Fig. S2 *A* and *B*). Individual layers are characterized by distinct crystal types. Thin sections of fossil shells show similar crystal form, attesting to the preservation of primary structure (Fig. S3).

Clumped Isotope Measurements. We measured the Δ_{47} of Gastropod shells from the Hampshire Basin during two sessions in late August to October 2010 and January 2011. Δ_{47} measurements followed procedures modified from those outlined in Ghosh et al. (10). Run conditions varied between the two periods, and Δ_{47} values were normalized relative to the Absolute Reference Frame (ARF) of Dennis et al. (11), using interlaboratory standards, equilibrated gases, and heated gases run during each period.

To determine Δ_{47} of shell carbonate, ∼5–10 mg of clean, powdered carbonate was loaded in a stainless steel sample "boat" and placed in a multisample carousel and reacted with anhydrous phosphoric acid held at 75 °C for 45 min in a common acid bath on an extraction line at the University of Michigan. The CO_2 generated during acid digestion was isolated and purified three times by quantitative cryogenic separation. The purified CO_2 gas was further cleaned by entraining it in a He stream and passing it through a 0.53-μm ID Supelco gas chromatography column held at −20 °C (modified from Ghosh et al.) (10) and was trapped cryogenically for 45 min. The collected sample gas was measured against gas of known composition on a Thermo Finnigan MAT 253 mass spectrometer at the University of Michigan with sample and reference capillaries balanced at a 16-V signal. Each sample and standard were measured over 10 cycles a total of 8–10 times. Total analysis time was 2.5–3 h.

Raw Δ_{47} values were determined using methods outlined by Eiler and Schauble (12), normalized through analysis of CO_2 gas with a range of isotopic compositions, and heated for a period of 2 h at 1,000 °C to achieve near stochastic distribution of isotopologue species. Individual instruments show varying degrees of "compression" of the Δ_{47} scale that can impact interlaboratory comparison and appropriate application of temperature-dependent equations. Measurement of Hampshire Basin samples predated the establishment of the Absolute Reference Frame (11), which uses CO_2 gas heated to 1,000 °C and gas with varied compositions equilibrated with water at 25 and 50 °C to account for scale compression of individual instruments. As a result, we corrected for scale compression on the University of Michigan (UM) instrument during each run period by using heated gases, an interlaboratory standard (UM Carrara), and CO_2 equilibrated with water at 25 °C for 48 h.

Series A in August–October 2010 (data file) was normalized by comparing the measured value of the intercept of the line defined by gases heated to 1,000 °C for 2 h relative to the working gas (−0.8442) and the mean measured value of UM Carrara marble that was reacted at 25 °C (−0.497) against the accepted values (11) (Fig. S4 *A* and *B*). Series B in January 2011 (data file) was normalized for instrumental scale compression by comparing the intercept of the line defining CO_2 gas heated to 1,000 °C for 2 h and CO_2 of varying isotopic compositions equilibrated with water at 25 °C for 48 h (Fig. S5 *A* and *B* and Table S2). All ongoing measurements at UM are normalized after Dennis et al. (11).

Individual samples were reacted at 75 °C and are corrected for this reaction temperature on the basis of empirical study of the impact of temperature on acid fractionation and Δ_{47}. The reaction of phosphoric acid with carbonate produces CO_2 gas. Because one oxygen atom from the original carbonate ion is lost during the reaction, the evolved gas is fractionated relative to the bulk carbonate species. The magnitude of isotopic fractionation is temperature dependent. The empirical temperature–Δ_{47} relationship was determined for materials reacted at 25 °C. Because our acid reaction was conducted at 75 °C in a common acid bath, it is critical to correct for the fractionation imparted by this temperature difference. We reacted three carbonates at temperatures of 25 °C, 50 °C, 60 °C, 75 °C, and 90 °C and measured in triplicate to determine temperature dependence on acid fractionation of Δ_{47}. Normalized data show that Δ_{47} values of carbonates reacted at 75 °C are 0.0670 lower than for samples reacted at 25 °C. Samples reacted at 90 °C have a Δ_{47} value 0.0807 lower than if reacted at 25 °C. Theoretical considerations suggest that the deviation between samples reacted at 90 °C and those reacted at 25 °C is 0.0781. We applied our empirically determined correction for 75 °C to the sample data, which averages a correction of 0.067‰.

Normalization of the data for scale compression relative to the ARF and correction for acid fractionation in this manner produce a mean Δ_{47} value for UM Carrara of 0.397 ± 0.007 during series A. This value includes samples reacted at 25 °C and 75 °C, attesting to the validity of the calibration during this period. Normalization of series B data relative to the ARF produces a mean Δ_{47} value for UM Carrara of 0.406 ± 0.007. This run includes UM Carrara samples reacted at temperatures of 75 °C and 90 °C and corrected for the temperature of reaction. Current normalization procedures for Δ_{47} measurements at the University of Michigan are based on measurement of gases heated to 1,000 °C for 2 h and CO_2 equilibrated with water at 25 and 50 °C and determination of

a common slope to account for instrumental scale compression. Comparison with inter- and intralaboratory working standards and samples shows no difference between ARF-normalized values during series A and B runs and current work at UM. Measured Δ_{47} values were converted to temperature, using the temperature-dependent equation established at California Institute of Technology, and adjusted to the ARF (11).

Temperature Dependence of Gastropod Growth Rate. Gill-breathing aquatic gastropods can grow over a wide range of temperatures and water chemistries, with some species tolerating prolonged temperatures in excess of 37–40 °C (13, 14). In modern temperate lakes, *Viviparus* show minimal growth during the cool autumn and winter months of September to March and rapid growth during the early spring period of May and June in response to increased temperatures and food availability as photosynthetic rates spike in lakes (15). Wintertime growth is virtually flat. Although snail migratory patterns are not universal, population study of *Viviparus georgianus* shows that these organisms live in an average habitat depth of 3 m during the winter and early spring months, migrating to shallower depths (1–3 m) during late spring in advance of the development of stratified lake conditions. In the autumn, organisms migrate again to deeper waters (2–4 m) as the lake turns over and stratification disappears. Collinson (3) suggested that water depths in the plant-bearing units of the Bembridge Marls Member were deposited at depths of less than 3 m (3) so snails likely record the upper, unstratified, oxygenated surface waters.

Determining the period of gastropod growth and carbonate mass accumulation in the gastropod shell is critical to relating Δ_{47}-derived temperature estimates to seasonal water temperature and mean annual climate. This is because Δ_{47} measurements require relatively large quantities of carbonate, which limits the ability to conduct high-resolution sampling of individual growth laminae on fossil gastropod shells. To address this, we examined temperature controls of gastropod growth. Studies show that the metabolic rate of freshwater fluvial and lacustrine male prosobranch gastropods is directly dependent upon temperature (16). In turn, shell growth rate is related to oxygen demand. The form of temperature dependence for male gastropods appears linear, whereas for female gastropods this approaches an exponential form that can be described by a van't Hoff's equation, potentially enabling male gastropods to survive over a larger temperature range. We used the empirical measures of temperature dependence of oxygen demand for male prosobranch gastropods to examine annual changes in metabolic rate due to changing water temperature and ultimately provide a conservative estimate of metabolic rate and potential carbonate mass accumulation over an annual cycle. Data from growth experiments conducted over a temperature range from 12 to 32 °C for prosobranch gastropods show that oxygen demand increases by a factor of 10 over this 20 °C range (16). The Late Eocene climate of the Hampshire Basin has been argued to be similar to the modern climate of the Florida Everglades (e.g., ref. 3). This is supported by paleosols that show evidence for marshy, poorly drained sediments and periodically flooded soils (2, 17) and flora of the Solent Group that represent freshwater marsh, pond, and lake plants with brief intervals that include a few floral components with lower water demands and brackish rather than freshwater biota (3). Flora from the Bembridge Marls Member reflect a *Typha*/*Acrostichum* marsh with areas of open water with rich wetland flora and free-floating vegetation (e.g., *Azolla*, *Stratiotes*, and waterlilies) and depths of less than ~3 m (3).

Using modern monthly shallow water temperature data from Volusa County, Florida (US Geological Survey Water Resource Data, http://waterdata.usgs.gov/nwis/sw), we calculated average monthly oxygen demand in response to seasonal changes in lake water temperature. These data suggest peak carbonate mass accumulation occurs during the warm summer months, with the June to September period accounting for nearly 50% of shell growth, and the months of April to October accounting for more than 75% of total mass accumulation (Fig. S6). Female gastropods show even greater temperature dependence on oxygen demand. These organisms might record even greater weighting of growth to the summer period. Modern *Viviparus* from controlled growth studies in the significantly cooler climate of the United Kingdom (18) also show the bulk of shell mass accumulates during the spring and summer period. This growth pattern likely reflects a combination of temperature and nutrient/food-related controls on growth. As a result, we suggest that Δ_{47} temperatures of ancient *Viviparus* fragments reflect spring to autumn water temperatures and are biased toward peak summer conditions. On the basis of temperature-dependent weighting of carbonate mass accumulation, the mean weighted time of shell carbonate accumulation would reflect a late July time average. To relate bulk shell Δ_{47} temperature to climate we use modern lake temperature–air temperature relationships (19).

Water Temperature–Mean Annual Air Temperature Transfer Functions. To relate gastropod Δ_{47} temperature data to broader climatic data, we use transfer functions that relate modern surface water temperatures for several different growing season scenarios (e.g., April to June, April to October, and June to August) with mean annual air temperature data (19). Because the absolute seasonally weighted gastropod carbonate temperature is unknown and our records provide some integrated signal from these months, these scenarios provide a means of understanding how growing-season water temperature relates to mean annual air temperature changes. This allows direct comparison with sea surface temperature records and paleoclimate model results. In all three scenarios of carbonate-mass integrated growth, water surface temperature data are strongly correlated with mean annual air temperature (19). The offset between integrated growing-season water temperature and mean annual air temperature is greatest in the case where the gastropod shells integrate the shortest time period of peak summer warmth; however, the equations for all three scenarios are broadly similar.

Eocene–Oligocene gastropod Δ_{47} water temperature data are converted to air temperature estimates, using these three estimated periods of seasonally weighted growth. All show that high Δ_{47} temperature data (i.e., >30 °C) are reflective of climatic conditions where mean annual air temperature (MAAT) (°C) is below 25 °C. These estimates are in solid agreement with paleofloral assemblages (20). Using integrated growth season water temperature–air temperature relationships, we calculate the expected MAAT (°C) across the Eocene–Oligocene transition (EOT), using gastropod Δ_{47} water temperature data. Growing season temperature was related to mean annual air temperature on the basis of the assumption that shell carbonate reflects integration of an April to October signal, according the equation

$$\mathrm{MAAT}(^{\circ}\mathrm{C}) = -0.0146 \times \mathrm{T}^2 + 1.753 \times \mathrm{T} - 16.079.$$

For all three scenarios (19), where gastropod growth evenly integrates April to October conditions, April to June conditions, or June through August conditions (peak water temperatures), reconstructed temperature change across the EOT is very similar (Table 1 in main text). Thus, regardless of whether gastropod growth integrates April to October conditions or June to August conditions, the implications for overall mean annual air temperatures are nearly identical. These all show a large temperature drop from the Late Eocene to Early Oligocene in growing-season water temperature and mean annual air temperature.

1. Hooker JJ, Grimes ST, Mattey DP, Collinson ME, Sheldon ND (2009) Refined correlation of the UK Late Eocene-Early Oligocene Solent Group and timing of its climate history. *GSA Spec Pap* 452:179–195.
2. Hooker JJ, Collinson ME, Sille NP (2004) Eocene-Oligocene mammalian faunal turnover in the Hampshire Basin, UK: Calibration to the global timescale and the major cooling event. *J Geol Soc London* 161(2):161–172.
3. Collinson ME (1983) Palaeofloristic assemblages and palaeoecology of the Lower Oligocene Bembridge Marls, Hamstead Ledge, Isle of Wight. *Bot J Linn Soc* 86(1–2):177–205.
4. Gale AS, et al. (2006) Correlation of Eocene-Oligocene marine and continental records: orbital cyclicity, magneto- and sequence stratigraphy of the Solent Group, Isle of Wight, UK. *J Geol Soc London* 163:401–415.
5. Sille NP, Collinson ME, Kucera M, Hooker JJ (2004) Evolution within the charophyte genus Harrisichara, late Paleogene, southern England; environmental and biostratigraphic implications. *Palaeogeogr Palaeoclimatol Palaeoecol* 208(1–2):153–173.
6. Pälike H, et al. (2006) The heartbeat of the Oligocene climate system. *Science* 314(5807):1894–1898.
7. Berggren WA, Kent DV, Swisher CC, III, Aubry M-P (1995) A revised Cenozoic geochronology and chronostratigraphy. *Geochronology, Time Scales and Global Stratigraphic Correlation*, SEPM Special Publication, eds Berggren WA, Kent DV, Aubry M-P, Hardenbol J (Society for Sedimentary Geology, Tulsa, OK), Vol 54, pp 129–212.
8. Coxall HK, Wilson PA, Pälike H, Lear CH, Backman J (2005) Rapid stepwise onset of Antarctic glaciation and deeper calcite compensation in the Pacific Ocean. *Nature* 433(7021):53–57.
9. Pearson P, et al. (2008) Extinction and environmental change across the Eocene-Oligocene boundary in Tanzania. *Geology* 36:179–182.
10. Ghosh P, et al. (2006) 13C-18O bonds in carbonate minerals: A new kind of paleothermometer. *Geochim Cosmochim Acta* 70:1439–1456.
11. Dennis KJ, Affek HP, Passey BH, Schrag DP, Eiler JM (2011) Defining an absolute reference frame for 'clumped' isotope studies of CO2. *Geochim Cosmochim Acta* 75:7117–7131.
12. Eiler JM, Schauble EO (2004) O-18–C-13–O-16 in Earth's atmosphere. *Geochim Cosmochim Acta* 68:4767–4777.
13. Miranda NAF, Perissinotto R, Appleton CC (2010) Salinity and temperature tolerance of the invasive freshwater gastropod *Tarebia granifera*. *S Afr J Sci* 106(3/4):1–7.
14. Ramakrishnan V (2007) Salinity, pH, temperature, desiccation and hypoxia tolerance in the invasive freshwater apple snail *Pomacea Insularum*. PhD dissertation (Univ of Texas, Arlington, TX).
15. Jokinen EH, Guerette J, Kortmann RW (1982) The natural history of an ovoviviparus snail, Viviparus georgianus (Lea), in a soft-water eutrophic lake. *Freshw Invertebr Biol* 1(4):2–17.
16. Buckingham MJ, Freed DE (1976) Oxygen consumption in the prosobranch snail *Viviparus Contectoides* (Mollusca: Gastropoda)—II. Effects of temperature and pH. *Comp Biochem Physiol A* 53(3):249–252.
17. Sheldon ND (2009) Non-marine records of climatic change across the Eocene-Oligocene transition. *GSA Spec Pap* 45:249–259.
18. Bugler MC (2011) An investigation into use of the freshwater gastropod Viviparus as a recorder of past climatic change. PhD thesis (Univ of Plymouth, Plymouth, UK). Available at http://pearl.plymouth.ac.uk/handle/10026.1/531.
19. Hren MT, Sheldon ND (2012) Temporal variations in lake water temperature: Paleoenvironmental implications of lake carbonate $\delta^{18}O$ and temperature records. *Earth Planet Sci Lett* 337:77–84, 10.1016/j.epsl.2012.05.019.
20. Eldrett JS, Greenwood DR, Harding IC, Huber M (2009) Increased seasonality in the latest Eocene to earliest Oligocene in northern high latitudes. *Nature* 459: 969–973.

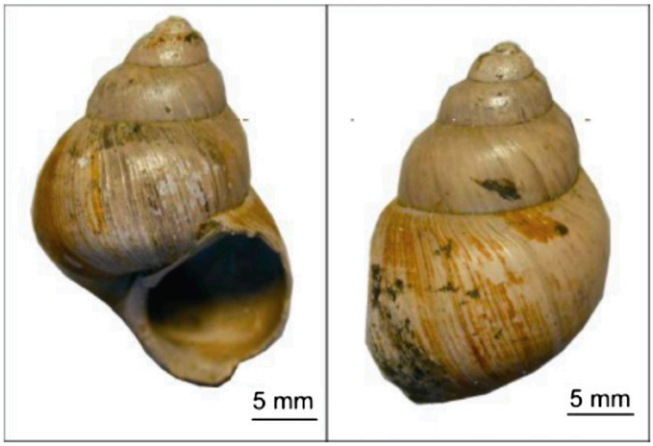

Fig. S1. Photograph of Late Eocene shell of *Viviparus*. Fossil shell is pristine and composed of primary aragonite (modified from Bugler, ref. 18).

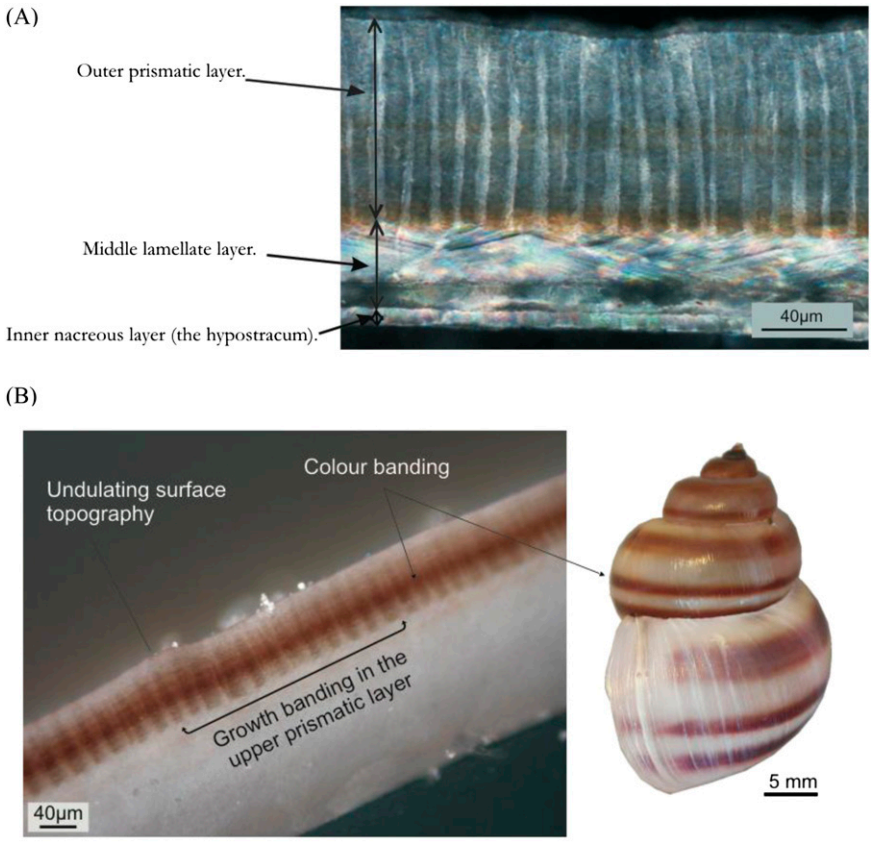

Fig. S2. (*A*) Thin section of a modern *Viviparus contectus* shell observed under cross-polarized light. The image reveals three calcareous layers with their individual crystal structures. The periostracum has been removed using NaClO. (*B*) Reflected light image of a cross section of a *V. contectus* shell showing the prismatic layer containing growth banding, which is colored brown by one of the three colored bands (modified from Bugler, ref. 18).

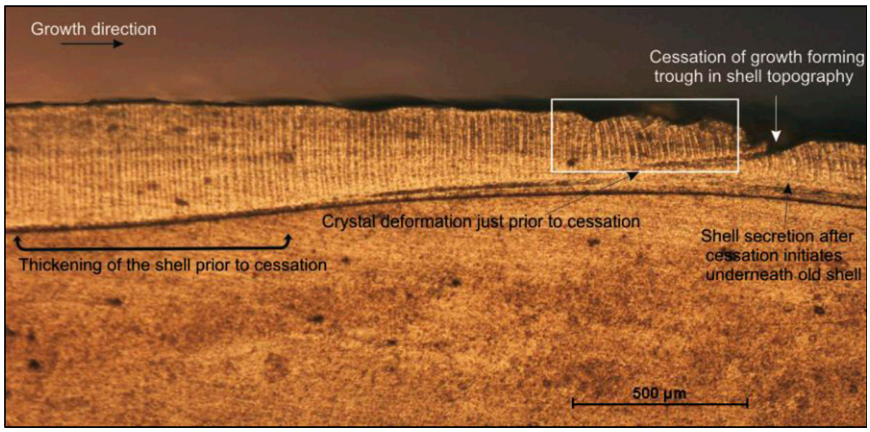

Fig. S3. Reflected light image of a polished cross section of fossil *Viviparus* showing that shell thins toward the point of growth cessation. The crystal structure in the thinner shell just before cessation has an erratic crystal structure. A topographic low occurs due to the newly secreted shell initiating underneath the old shell (modified from Bugler, ref. 18).

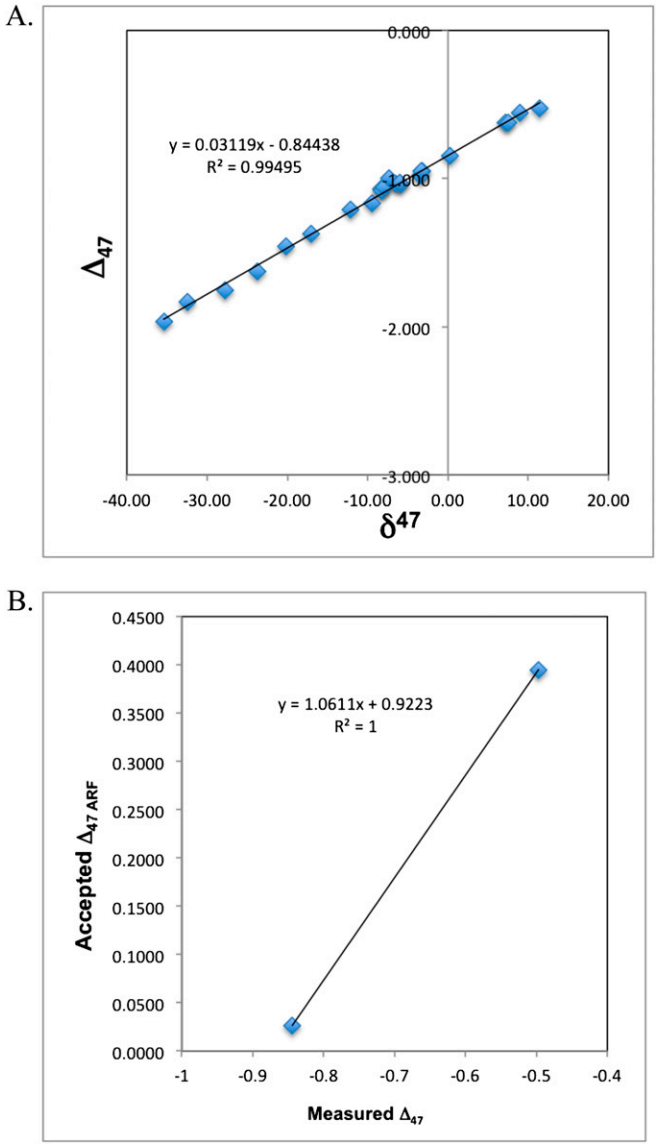

Fig. S4. (*A*) Heated gas line for series A for determination of Δ_{47} values. (*B*) Transfer function relating measured Δ_{47} value of UM Carrara and the intercept of the heated gas line and the accepted values relative to the Absolute Reference Frame of Dennis et al. (11).

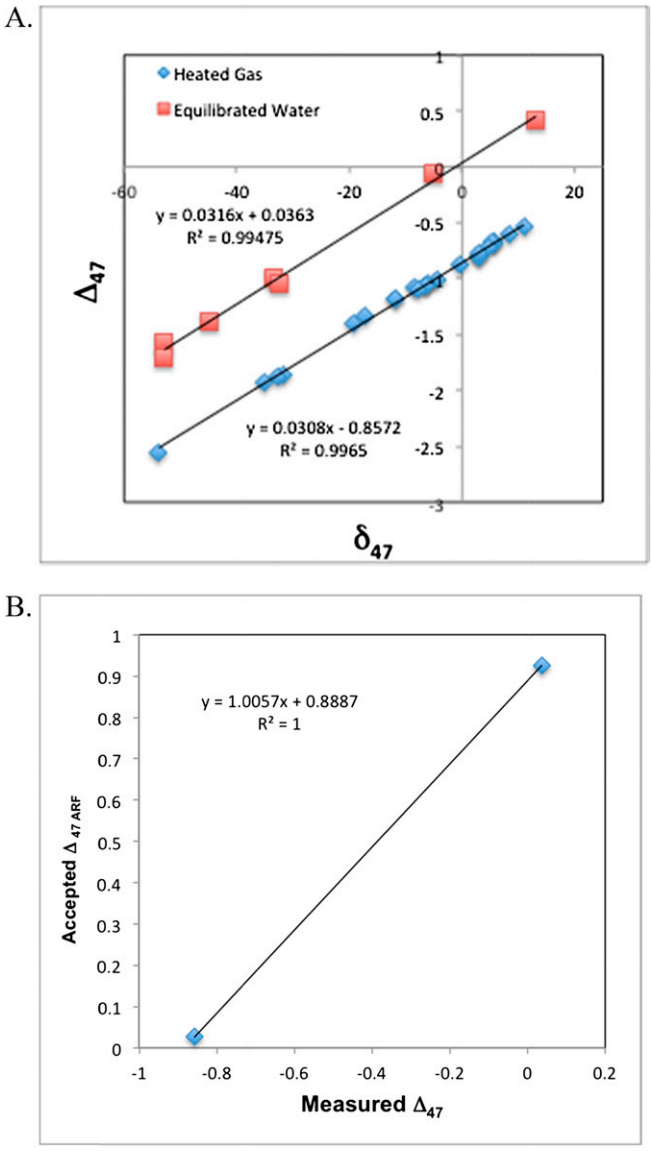

Fig. S5. (*A*) Heated gas line and CO_2 equilibrated with water at 25 °C for series B for determination of Δ_{47} values. (*B*) Transfer function relating measured Δ_{47} value of the intercept of the line defining CO_2 equilibrated with water at 25 °C and the intercept of the heated gas line and the accepted values relative to the Absolute Reference Frame of Dennis et al. (11).

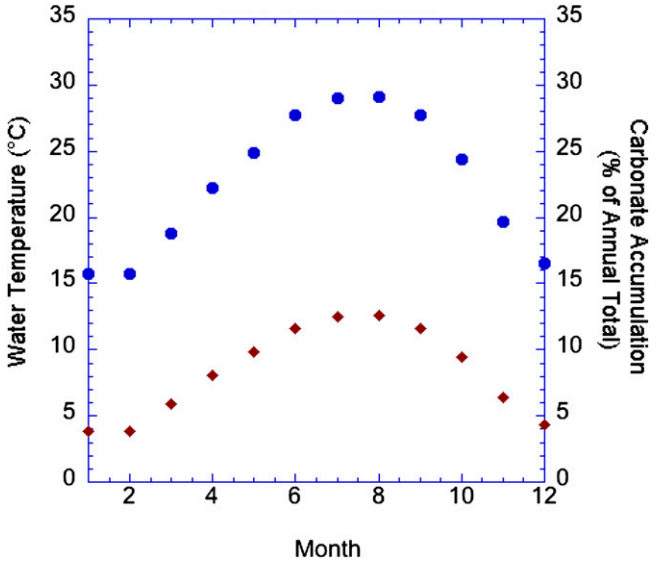

Fig. S6. Estimated percentage of total carbonate mass accumulation for Florida Everglades aquatic gastropods based on linear temperature dependence for oxygen demand and monthly water temperature data. Blue dots represent water temperature and brown diamonds represent carbonate accumulation.

Table S1. Stable isotope results for Isle of Wight gastropods

Sample name	Unit	Level/ thickness, m	Age, Ma	$\delta^{13}C$ (VPDB), ‰	$\delta^{18}O$ (VPDB), ‰	$\delta^{18}O_{water}$ (VSMOW), ‰	$\Delta_{47\ ARF}$[†]	T, °C*,[†]
TBC S2-1				−4.0	−0.5	0.6	0.738	19
TBC S2-2				−3.9	−0.1	1.0	0.686	30
TBC S2-3				−4.0	−0.2	0.9	0.715	24
TBC S2-4				−3.9	−0.1	1.0	0.728	22
TBC S2	**Cranmore**	**1.8/9.5**	**32.41**	**−4.0**	**−0.2**	**0.9**	**0.717 ± 0.011**	**24 ± 2**
BOULD S5-1				−0.7	−0.2	−1.4	0.725	22
BOULD S5-2				−0.6	−0.2	−1.3	0.735	20
BOULD S5-3				−0.7	0.1	−1.0	0.744	18
BOULD S5	**Upper Hamstead**	**2.2/60**	**33.25**	**−0.7**	**−0.1**	**−1.2**	**0.735 ± 0.010[‡]**	**20 ± 2[‡]**
BOULD S1-1				−3.6	−1.5	1.1	0.656	37
BOULD S1-2				−3.4	−1.4	1.3	0.752	17
BOULD S1-3				−3.5	−0.7	1.9	0.681	31
BOULD S1-4				−3.5	−1.4	1.2	0.655	37
BOULD S1-5				−4.4	−1.2	1.5	0.653	38
BOULD S1	**Lower Hamstead**	**9.25/11**	**33.71**	**−3.7**	**−1.2**	**1.5**	**0.679 ± 0.018**	**32 ± 4**
HAM S13-1				−3.2	−1.3	−0.6	0.722	23
HAM S13-2				−3.0	−0.6	0.0	0.728	21
HAM S13	**Lower Hamstead**	**7.9/11**	**33.75**	**−3.1**	**−1.0**	**−0.3**	**0.725 ± 0.012[‡]**	**22 ± 2**
HAM S5-1				−2.9	−1.6	1.3	0.682	31
HAM S5-2				−2.9	−1.5	1.4	0.670	34
HAM S5	**Lower Hamstead**	**0.3/11**	**33.84**	**−2.9**	**−1.5**	**1.3**	**0.676 ± 0.012[‡]**	**33 ± 3[‡]**
HAM S7-1				−4.1	−0.8	1.8	0.666	35
HAM S7-2*				−4.1	−0.5	2.1	0.711	25
HAM S7-3				−4.3	−0.9	1.7	0.695	28
HAM S7	**Bembridge Marls**	**11.6/25.45**	**34.05**	**−4.2**	**−0.9**	**1.7**	**0.681 ± 0.012**	**32 ± 3**
HAM S-2–1				−2.9	−1.8	0.2	0.697	28
HAM S-2–2				−3.1	−2.3	−0.3	0.729	21
HAM S-2–3				−3.0	−2.0	0.0	0.666	35
HAM S-2	**Bembridge Marls**	**5.9/25.45**	**34.16**	**−3.0**	**−2.1**	**0.0**	**0.697 ± 0.016**	**28 ± 4**
BEMB S3-1				−3.4	0.3	3.3	0.663	35
BEMB S3-2				−3.7	−0.1	2.8	0.680	32
BEMB S3	**Seagrove Bay**	**8.65/8.7**	**34.37**	**−3.5**	**0.1**	**3.1**	**0.671 ± 0.012[‡]**	**34 ± 3[‡]**
SCO S4-1				−3.5	−2.7	−0.7	0.677	32
SCO S4-2				−3.4	−2.3	−0.2	0.710	25
SCO S4	**Fishbourne**	**1.97/2**	**34.8**	**−3.4**	**−2.5**	**−0.4**	**0.693 ± 0.017**	**29 ± 4**
SCO S6-1				−4.6	−1.9	0.6	0.703	27
SCO S6-2				−4.3	−1.4	1.1	0.682	31
SCO S6-3				−4.5	−2.2	0.3	0.665	35
SCO S6-4				−4.4	−1.4	1.6	0.679	32
SCO S6	**Lacey's Farm**	**2.8/3.1**	**35**	**−4.4**	**−1.7**	**0.7**	**0.682 ± 0.008**	**31 ± 2**

Bold rows indicate the mean of the values for the sample. VPDB, Vienna pee dee belemnite; VSMOW, Vienna standard mean ocean water.
*Temperature calculation using Δ_{47} temperature calibration of Ghosh et al. (10) and revised for ARF in Dennis et al. (11).
[†]SE denotes SEM of multiple splits except where noted.
[‡]For samples where SE of replicates was lower than the SE of the standard, SE was assigned using the long-term SD of a standard (Carrara, 0.017‰) divided by sqrt(n), where n is the number of sample replicates.

Table S2. Transfer function data for series A and series B

Transfer function	$\Delta_{47\ Raw}$	Accepted $\Delta_{47\ ARF}$
Series A		
Carrara Δ_{47}	−0.497	0.3950
Heated gas intercept	−0.8442	0.0266
Series B		
Gas equilibrated at 25 °C	0.0363	0.9252
Heated gas intercept	−0.8572	0.0266

Table S3. Monthly water temperature (Orange County, FL), temperature adjusted metabolic rate, and potential growth rate (carbonate mass accumulation) based on temperature dependence of metabolic rate (ref. 14)

Month	Water temperature, °C	Metabolic rate, units	Potential monthly mass accumulation, % of annual
January	15.7	0.027	3.8
February	15.7	0.027	3.8
March	18.8	0.041	5.9
April	22.2	0.056	8.1
May	24.9	0.068	9.8
June	27.7	0.081	11.6
July	29.0	0.087	12.5
August	29.1	0.087	12.5
September	27.7	0.081	11.6
October	24.4	0.066	9.5
November	19.7	0.045	6.4
December	16.5	0.030	4.4

Other Supporting Information Files

Dataset S1 (XLSX)